Hybrid nano-architectures loaded with metal complexes for the co-chemotherapy of head and neck carcinoma

Melissa Santi,[1,§] Valentina Frusca,[2,§] Maria Laura Ermini,[2] Ana Katrina Mapanao,[2,6] Patrizia Sarogni,[2] Alessandra Gonnelli,[2,3] Noemi Giannini,[2,3] Agata Zamborlin,[2,4] Lorenzo Biancalana,[5] Fabio Marchetti[5] and Valerio Voliani[2,*]

[1] NEST Istituto Nanoscienze-CNR and Scuola Normale Superiore, 56127, Pisa, Italy.

[2] Center for Nanotechnology Innovation@NEST, Istituto Italiano di Tecnologia, Piazza San Silvestro 12, 56127, Pisa, Italy.

[3] Radiation Oncology Unit, Pisa University Hospital, Via Roma 67, Pisa, Italy

[4] NEST-Scuola Normale Superiore, Piazza San Silvestro 12, 56127 Pisa, Italy

[5] Department of Chemistry and Industrial Chemistry, University of Pisa, Via Moruzzi 13, 56124 Pisa, Italy.

[6] Current address: Center for Radiopharmaceutical Sciences, Paul Scherrer Institute, 5232 Villigen-PSI, Switzerland.

[§]Equal contribution

*Corresponding author: valerio.voliani@iit.it

ABSTRACT

Head and neck squamous cell carcinoma (HNSCC) are a complex group of malignancies that affect different body sites pertaining to the oral cavity, pharynx and larynx. Their treatment relies on chemotherapy as neoadjuvant, adjuvant, and concomitant therapy to surgery and irradiation. The drugs of choice are platinum complexes, even if they exert severe side effects that can negatively affect prognosis. For this reason, other compounds are being investigated as alternatives or adjuvants to platinum complexes, which the major exponent being cisplatin. In this context, exploiting (supra)additive effects by the concurrent administration of cisplatin and emerging metal complexes is a promising research strategy that may lead to an effective cancer management with reduced adverse reactions.

Here, the combined action of cisplatin and a ruthenium(II) η^6-arene compound (RuCy), as both free molecules and loaded into hybrid nano-architectures (NAs), has been assessed on HPV-negative HNSCCs models of increasing complexity: 2D cells cultures, 3D multicellular tumor spheroids, and chorioallantoic membranes (CAMs). Two new NAs have been established to explore all the delivery combinations and compare their ability to enhance the efficacy of cisplatin in the treatment of HNSCCs. A significant supra-additive effect has been observed in both 2D and 3D models by one combination of treatments, suggesting that cisplatin is particularly effective when loaded on NAs, whereas RuCy performs better when administrated as a free compound. Overall, this work paves

the way for the establishment of the next co-chemotherapeutic approaches for the management of HNSCCs.

Keywords: oral malignancies, co-therapy, 3D models, ruthenium, cisplatin, nanoparticles

1. INTRODUCTION

Head and Neck Squamous Cell Carcinoma (HNSCC) is a complex group of epithelial malignancies that affect different body sites, among which the oral cavity, nasopharynx, oropharynx, larynx, and salivary glands.[1] HNSCC is mainly caused by extensive consumption of tobacco and alcohol, but recently a new subset of head and neck cancers, with peculiar biological and clinical features, was discovered to be associated to Human Papilloma Virus (HPV) infection.[2] HNSCC is one of the most common cancer worldwide, with more than 900.00 new cases and 450.000 deaths in 2020, accounting for 6% of all cancers and just over 3% of all cancer deaths.[3]

The treatment approaches are associated with anatomical subsite, stage, disease characteristics, functional considerations and patient wishes. Although natural history is different for HPV-related than for tobacco-related HNSCC, and intensive therapy is more difficult in elderly patients.[4] The current standards of care for HNSCC patients include surgery and radiotherapy, followed by chemotherapy.[5] When surgical resection is less feasible or would result in poor long-term functional outcomes, chemo-radiotherapy is the curative standard of care.[6] In these patients, high-dose cisplatin (100 mg/m^2 of body-surface area, administered intravenously every 21 days for three cycles) concurrently with radiotherapy is the standard of care with established survival benefits for patients with good performance status. However, because of substantial short- and long-term toxic effects associated with cisplatin, its use is predominantly reserved for nonelderly patients who have no major coexisting conditions. For less fit patients and patients in whom high-dose cisplatin is associated with unacceptable adverse effects, alternative systemic therapies are under investigation.[6]

The combination of chemotherapeutic agents may result in an improved efficacy of the treatment of malignancies compared to the effects of a single agent. The additive or synergistic effects of multiple agents usually lead to noticeably higher clinical benefit.[7] In this scenario, adjuvant drugs are increasingly demanded to reduce the adverse reactions associated to the cisplatin chemotherapy doses.

Recently, the chemistry of ruthenium complexes has received increasing interest due to the potential anticancer behavior of many derivatives. Some ruthenium-based anticancer metallotherapeutics have demonstrated an activity against some cisplatin resistant cell lines and less severe side effects compared to cisplatin and derivatives.[7] The low toxicity of ruthenium(III) complexes is associated with the ability of the metal to bind iron-binding serum protein, localizing the therapeutic action in the target.[8]

To date, only a handful of ruthenium(III) therapeutics has entered clinical trials but have not yet initiated or

completed a phase II study. Since the mode of action of these compounds is supposed to involve ruthenium(III) to ruthenium(II) reduction in the tumor environment, Ru(II) complexes have bee intensively investigated and [$RuCl_2$(PTA)(η^6-*p*-cymene)], comprising the amphiphilic phosphine 1,3,5-triaza-7-phosphatricyclo[3.3.1.1]decane (PTA) and known as RAPTA-C, emerged as promising (**Fig. S1A**).[9] RAPTA-C acts on the angiogenesis processes of tumors (not on necrosis/apoptosis), reducing the formation of new vessels and limiting the access of malignant cells to oxygen and nutrients.[10,11] Recently we developed new robust ruthenium(II) arene complexes and their activity were tested in 3D models of ± HPV HNSCC cell lines.[12] This series of compounds is formed by cationic ruthenium(II) p-cymene complexes bearing α-diimine ligands, of general formula [RuCl{κ^2*N*-(HC=NR)$_2$}(η^6-*p*-cymene)]NO_3, and show high stability in biological media and good solubility in water.[13,14] In particular, RuCy (R = cyclohexyl, **Figure S1B**), showed a good toxic activity on HNSCCs cell lines with an IC_{50}<100 μM at 72h after treatment (2 h exposure to the drug).[12]

In general, ruthenium complexes result interesting alternatives to cisplatin as well as potential adjuvants in co-chemotherapy approaches. Noticeably, very few studies explored the combined effect of cisplatin and other metal complexes in the treatment of neoplasms.[15]

Here, the combinatorial effect of cisplatin and RuCy has been evaluated on models of HPV-negative HNSCCs of increasing complexity. In particular, we evaluated three different delivery approaches for the simultaneous administration of cisplatin and RuCy: i) as free compounds, ii) both included in a specifically designed hybrid nanoarchitecture (NAs), and iii) in a mixed strategy including free RuCy and cisplatin loaded into NAs. NAs are hybrid nano-architectures composed by biodegradable silica capsules containing a polymeric matrix and ultrasmall metal nanoparticles.[16] The extreme versatility of the synthetic protocol allows for the loading of active molecules in the inner cavity as well as for surface functionalization.[17,18] The NAs family has been developed to avoid the issue of plasmon nanomaterial persistence after the action with a special focus in oncology.[19,20] The combinatorial effect of the three strategies has been assessed on 2D cells cultures, 3D multicellular tumor spheroids, and chorioallantoic membranes (CAMs) in agreement to the European Parliament Directive 2010/63/EU. CAMs are *in vivo* alternative models for the reliable evaluation of innovative approaches for cancer detection and treatment.[21] Indeed, the highly vascularized membrane of CAMs can be exploited to support the development of tumor xenografts and to explore the angiogenesis-related mechanisms and/or the anti-metastatic/antitumor activity of the treatments.[18,22]

Overall, our investigation denotes that co-chemotherapy based on nanomaterials is a promising strategy for the cancer management and that the employment of alternative *in vivo* models is crucial in oncological preclinical research.

2. MATERIALS AND METHODS

2.1 Synthesis of gold nanoparticles.

All nanoparticles were formulated starting from a standard protocol for NAs synthesis as described previously.[16] Briefly, ultrasmall gold nanoparticles with diameter of approximately 3 nm were prepared by adding 20 µl of poly(sodium 4-styrene sulfonate) (PSS, 30% aqueous solution) and 200 µL of $HAuCl_4$ aqueous solution (10 mg/mL) to 20 mL of milliQ® water. During stirring, 200 µL of sodium borohydride (8 mg/mL in milliQ water) were added quickly to the mixture that was mixed for another 2 minutes. The solution was aged 10 minutes at room temperature and became brilliant orange.

2.2 Synthesis of drug-loaded nano-architectures (NAs)

NAs-CisPt and NAs-CisPt-Rucy gold aggregates were prepared using a modified poly(L-Lysine) loaded with cisplatin prodrug, synthesized as described below.

2.2.1 Synthesis of c,t,c-$[PtCl_2(OH)_2(NH_3)_2]$. The method was based on what was previously described by Hall *et al*.[23] Powder of cis-$[PtCl_2(NH_3)_2]$ (0.40 g, 1.33 mmol) was suspended in milliQ® water (10 mL) and H_2O_2 30% (w/v) (14 mL, ten-fold excess) was added. The mixture was mixed for 1 h at 50°C. Then it was cooled in ice to reach 0°C and saturated water solution of NaCl (10 mL) was added. The resultant pale yellow powder was filtrated and washed with cold water and ethanol, and dried in a vacuum pump, yielding c,t,c-$[PtCl_2(OH)_2(NH_3)_2]$ (223 mg, 0.67 mmol, 50%).

2.2.2 Synthesis of c,t,c-$[PtCl_2(NH_3)_2(OH)(O_2CCH_2CH_2CO_2H)]$. We used a modified method already described elsewhere.[24] c,t,c-$[PtCl_2(OH)_2(NH_3)_2]$ (0.2 g, 0.6 mmol) was suspended in anhydrous dimethyl sulfoxide (DMSO, 16 mL) and succinic anhydride (0.06 g, 0.6 mmol) was added to the solution and stirred at room temperature for 12 h. The solution was freeze-dried and acetone (10 mL) was added to precipitate a light yellow solid, which was collected by filtration and washed several times with acetone, diethyl ether, and then dried in a vacuum pump, yielding c,t,c-$[PtCl_2(NH_3)_2(OH)(O_2CCH_2CH_2CO_2H)]$ (0.16 g, 0.37 mmol, 62%).

2.2.3 Synthesis of Drug-Modified Poly(L-Lysine) (PL-CisPt). 0.5 mg of c,t,c-$[PtCl_2(NH_3)_2(OH)(O_2CCH_2CH_2CO_2H)]$ powder was dissolved in 400 µL of PBS buffer and mixed with freshly made EDC/NHS (40 µL, 0.21 M) milliQ® water solution (EDC: N-(3-dimethylaminopropyl)-N0-ethylcarbodiimide hydrochloride, NHS: N-hydroxysuccinimide). The mixture was stirred 10 minutes at room temperature and then poly(L-lysine) hydrobromide 15–30 kDa (75 µL, 20 mg/mL milliQ® solution) was added to the reaction. The resulting solution was stirred overnight at room temperature. The modified poly(L-lysine) was collected and washed three times with PBS buffer by Amicon 10kDa filter units, and then dissolved in PBS buffer (800 µL).

2.2.4 Synthesis of NAs-CisPt aggregates.

NAs-CisPt aggregates were synthesized starting from a 20 mL aqueous solution of ultrasmall gold nanoparticles. 165 µL of PL-CisPt was slowly added to the solution, then stirred 20 minutes at room temperature. Aggregates were collected by centrifugation (13,400 rpm for 3 min) and resuspended in 2 mL of milliQ® water. The solution was sonicated for a maximum of 4 minutes to resuspend aggregates.

2.2.5 Synthesis of NAs-CisPt-RuCy aggregates.

NAs-CisPt-RuCy aggregates were also synthesized starting from a 20 mL aqueous solution of ultrasmall gold

nanoparticles added with 210 µL of a solution of RuCy (24 mg/mL in milliQ®:DMSO, 1:2). Upon addition of RuCy, the reaction mixture turned from brilliant orange to brown. Then 75 µL PL were added to the solution that was allowed to stir at room temperature for 20 minutes and then centrifuged to collect aggregates. The arrays were suspended in 2 mL of milliQ® water and sonicated for a maximum of 4 minutes.

2.2.6 Synthesis of NAs-RuCy aggregates.

NAs containing no gold nanoparticles were also synthesized starting from a solution of 20 mL milliQ water and 10 µL PSS by adding first 210 µL of RuCy solution (24mg/ml in milliQ®:DMSO, 1:2), and then 75 µL PL. Arrays were collected by centrifugation and resuspended in 2 mL milliQ® water by sonication. The appearance of the reaction mixture shifted from colorless to yellow upon addition of RuCy.

2.2.7 Synthesis of complete nano-architectures.

The last step is the formation of the silica shell around aggregates that is the same for all the types of nanoparticles. We used a modified Stöber method as described below: 70 mL of absolute ethanol were mixed with 40 µL of tetraethyl orthosilicate (TEOS, 98%) and 2.4 mL of ammonium hydroxide solution (30% in water). Then, 2 mL of the gold nanoparticle arrays previously prepared were added to the mixture and the solution was allowed to gently shake at room temperature for 3 h (3.5 h for NAs-RuCy and NAs-CisPt-RuCy). The synthesized nanoarchitectures were collected by 30 min centrifugation at 4000 rpm, washed twice with ethanol and suspended in 1 mL of ethanol. A short spin centrifugation was employed in order to separate the structures with diameters larger than 150 nm from the supernatant. The solution containing about 1.5 mg of NAs was stored at −20°C until use. It remains usually stable for at least one year. All types of nanoparticles were fully characterized to verify the success of the synthetic process.

2.3 Dynamic Light Scattering (DLS) and Zeta-potential measurements

Measurements by DLS were performed at 37 °C in a 1 mL quartz cuvette on a Zetasizer nano-ZS90 (Malvern Instruments, Malvern, United Kingdom) following the manufacturer's instructions. Nanomaterials were diluted to 0.15X and suspended in PBS and analyzed with a single scattering angle of 90°. For the zeta-potential measurements the sample was transferred into DTS 1070 standard capillary cells. Each value reported is the average of four consecutive measurements.

2.4 UV–Vis Spectrophotometry

Extinction spectra were measured with a Mettler Toledo UV5 Nano spectrophotometer, using the micro-volume platform. Nanoparticles were dissolved in 1X PBS solution and an aliquot of 3 µL was used for the measurements.

2.5 Inductively coupled Plasma-Mass spectrometry (ICP-MS) analysis

An aliquot (10 µL) of the nanoparticles was placed in a pressure vessel and dissolved in 200 µL of aqua regia. The sealed vessel was placed in CEM Discover SP-D for further digestion under microwave irradiation (200°C/15 min). The sample was then diluted with 3% nitric acid to 4 mL. The amounts of elemental gold, platinum or ruthenium were determined after analysis on ICP-MS Agilent 7700 (Agilent Technologies, Santa

Clara, CA, USA), using standard calibration curves. A 10 ppm Hg solution in 3% nitric acid was used as internal standard.

2.6 Transmission electron microscopy characterization

The TEM observations of all nanoparticles were performed in ZEISS Libra 120 PLUS operating at 120 KV and equipped with an In-column Omega filter. The suspensions with the nanoparticles (5 µL) were deposited to a 300-mesh of carbon coated copper grids and let dry before image acquisition.

2.8 Release assay

An aliquot of 500 µL of NAs-RuCy was resuspended in 100 µL of HEPES buffer (20 mM, pH 7.4) and placed in a dialysis membrane (molecular weight cut-off: 10 kDa). The membrane was then placed in a 50-mL tube with 15 mL of HEPES buffer. The solution was maintained at 37 °C for 7 days. For every time point an aliquot (3 mL) of buffer was drawn and the ruthenium content was analyzed using ICP-MS.

2.9 Cell culture

SCC-25 cell line was purchased from American Type Culture Collection (ATCC) and cultured following manufacturer's instructions. Cells were maintained in a mixture of Dulbecco's modified Eagle and Ham's F12 (DMEM/F12 1:1) from Invitrogen (Carlsbad, CA, USA). The medium was also supplemented with 10% fetal bovine serum (FBS), 4 mM L-glutamine, 1 mM sodium pyruvate, 100 U/mL penicillin, 100 mg/mL streptomycin (Invitrogen) and 400 ng/mL of hydrocortisone (Merk). Cells were maintained at 37°C in a humidified 5% CO_2 atmosphere. For 3D models, we used a protocol previously described by us.[25] Briefly, cells were harvested and centrifuged for 5 min at 1200 rpm. Then, suspended in fresh medium, counted and the suspension was adjusted to a final concentration of 1×10^6 cells/mL. Then, 10 µL drops of cells suspension were placed on the lid of a 100-mm cell culture dish that was flipped into the chamber containing 10 mL of PBS to avoid drops dehydration. Drops were maintained in the incubator at 37°C, until cells formed a sheet and then were transferred to a 100 mm suspension culture dish after 3 days. Finally, cell aggregates were placed inside a CO_2 incubator with an orbital shaker (60-70 rpm) for 24 h to induce the formation of the final spherical conformation.

2.10 Viability assays

Viability on 2D cell cultures were evaluated for SCC-25 cell line after treatment with different combination of NAs and ruthenium arene complexes. In all cases, 10^4 cells/well were seeded in 96-well plates and growth for 24 h at 37°C and 5% CO_2. Then cells were treated for 2h at 37°C, washed twice with PBS and viability was measured at 24, 48 and 72h after treatments. Cytotoxicity was evaluated using a tetrazolium salt, 2-(2-methoxy-4-nitrophenyl)-3-(4-nitrophenyl)-5-(2,4-disulfophenyl)-2H tetrazolium, and monosodium salt (WST-8) assay (Tebu-Bio). For each experimental time point, cells were incubated with WST-8 reagent (10 µL) and medium (90 µL) for 2 h. Absorbance (450 nm) was measured using a microplate reader (Glomax Discovery, Promega, Madison, WI, USA). The percentage of cell viability was determined by comparing drug-treated cells with the untreated cells (100% viability). Viability of 3D spheroids was evaluated using CellTiter-Glo® 3D

Cell Viability Assay (Promega, Milan, Italy). Spheroids for each time point were transferred from a round-bottom 96-well plate to a white 96-well plate (one spheroid for one well in 100 µL of medium) for luminescence measurements. Then, 100 µL of CellTiter-Glo® 3D reagent was added to each well, the plate was shaken for 5 min and the luminescence signal was recorded after 25 min of incubation with a microplate reader (Glomax Discovery, Promega, Madison, WI, USA). Cell viability was determined with respect to the viability of spheroids maintained in complete medium without treatments. Data represent the average of three independent experiments. Error bars represent the SD from three independent experiments.

2.11 CAM assay

Red Leghorn chicken eggs were incubated at 37°C in a fan-assisted humidified egg incubator (FIEM). For detailed procedures please refer to the methods already published by our group.[22] Briefly, from Embryonic Day of Development 0 (EDD0) to EDD3 the eggs were positioned horizontally and rotated to allow the natural formation of the air chamber. On EDD3, a small hole was created on the blunt end of each egg with tweezers. The eggs were then positioned vertically and at EDD6 a small window of about 1 cm^2 was created to allow the grafting of 2 x 10^6 SCC-25 cells in cell culture medium and Matrigel (Corning, Ref 354234) with ratio 1:1. At EDD10 the tumor-bearing embryos were randomized and divided in different groups of treatment. 10 µg of RuCy complex was calculated for the treatment. The right amount of powder was dissolved in DMSO solution keeping the volume as low as possible to maintain a final % v/v of DMSO lower than 5% (this percentage is harmless for eggs, data not showed). An aliquot of NAs-CisPt was taken such that each tumor would also be treated with 4 µg of Pt per egg. Eggs were treated with RuCy alone, NAs-CisPt alone and RuCy and NAs-CisPt combined together. All materials were administered topically after resuspension in 30 µL of serum-free medium. Embryo viability and tumor size were monitored every two days and tumor volume was calculated using a modified ellipsoid formula: volume = ½ (length x $width^2$).[26] At EDD14, the chicken embryo movements were slowed down by hypothermia (2h at 4°C) and then the tumors were harvested. After 24h at 4°C, the organs (heart, liver, lungs) were collected from the embryos. Samples (tumors, organs) for ICP-MS were stored at -80°C until analysis.

3. RESULTS AND DISCUSSION

3.1 Synthesis and characterization of NAs-CisPt, NAs-RuCy and NAs-CisPt-RuCy

The nano-architectures have been synthetized by employing standard protocols[27] with some modifications due to the encapsulation of the ruthenium complex (NAs-RuCy) and of both the metallic-drugs (NAs-CisPt-RuCy). A schematic explanation of the steps involved in the synthesis is reported in **Figure 1A**. In general, a colloidal solution of ultrasmall gold nanoparticles (USNPs) is prepared in the presence of poly(sodium-4-styrene sulfonate) (PSS). Then, the USNPs are aggregated with poly-L-lysine (PL) in presence of the drugs, and the USNPs arrays are employed as templates for the composition of the silica nano capsules. In **Figure 1** are reported the standard characterizations for NAs-CisPt-RuCy while in **Figure S2** and **Figure S3** are reported the

characterization for, respectively, NAs-CisPt and NAs-RuCy. All diameters and zeta-potentials are reported in **Table 1**.

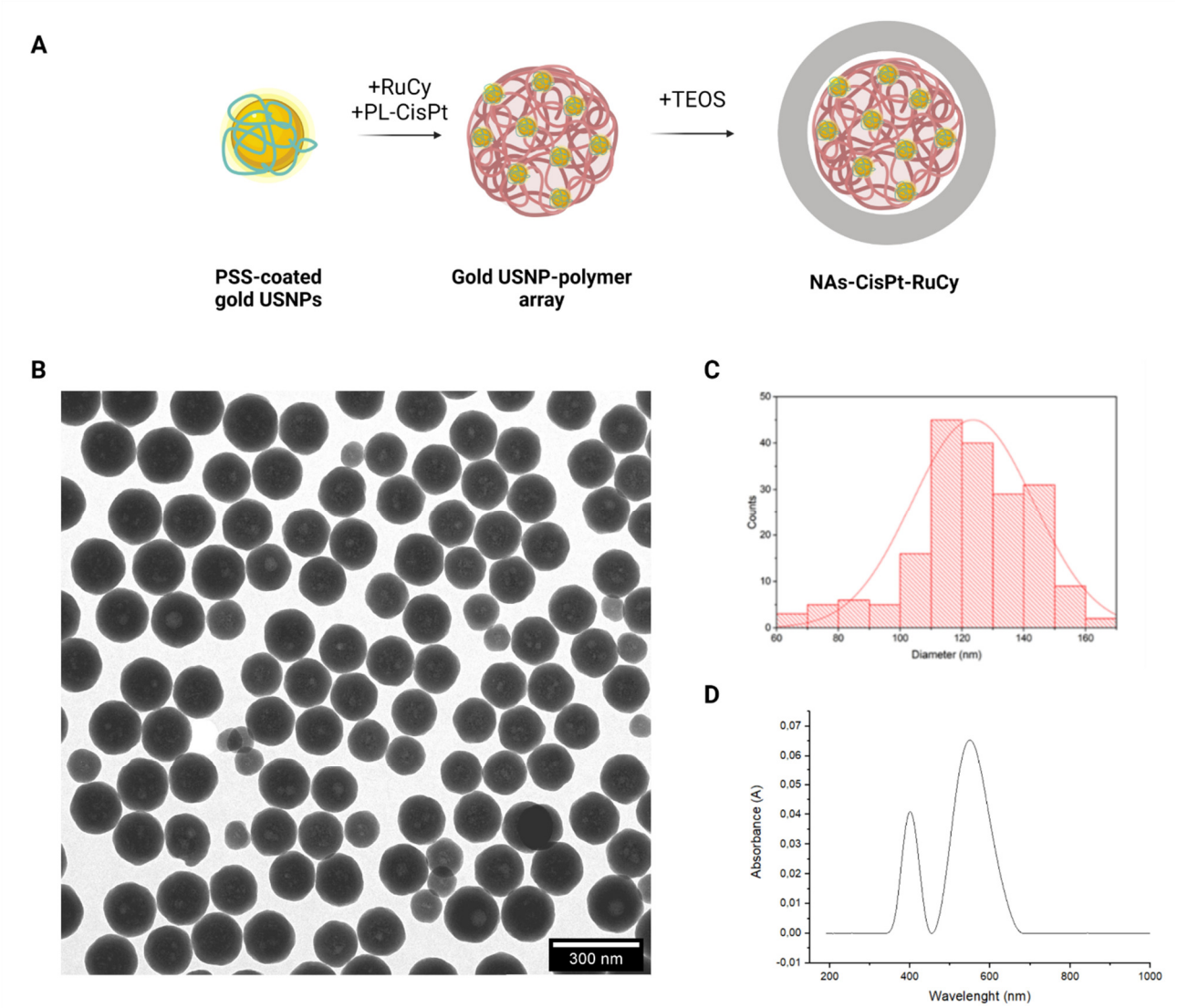

Figure 1: A) Schematic representation of the synthetic process for NAs-CisPt-RuCy. B) TEM images of NAs-CisPt-RuCy. Scale bar: 300 nm. C) Size histogram of NAs-CisPt-RuCy made on at least 100 NAs observed with TEM. The diameter of NAs was analyzed with ImageJ. D) Background subtracted UV-Vis spectrum of NAs-CisPt-RuCy.

Table 1: Physical-chemical characterization of the nano-architectures.

	Diameter in PBS (nm-DLS)	**Diameter (nm-TEM)**	**Zeta-Potential (mV)**
NAs-CisPt	227 ± 1	150 ± 26	-20 ± 1
NAs-RuCy	195 ± 9	138 ± 22	-19.3 ± 1.3

NAs-CisPt-RuCy	214 ± 19	138 ± 13	-21.0 ± 1.3

The ruthenium complex in NAs-RuCy is loaded with a non-covalent strategy (as opposite to cisplatin in NAs-cisPt), thus the release of the ruthenium compound from NAs-RuCy has been investigated. NAs-RuCy have been incubated in HEPES buffer at 37 °C for 7 days and for each time point an aliquot of buffer was drawn and analyzed by ICP-MS to measure the ruthenium content. The release profile suggested an exponential release in the first 100h followed by a plateau (**Figure S4A**), in agreement with the partial degradation of the silica capsules (**Figure S4B**) in buffers.[16]

3.2 2D viability assay

Cells have been treated with a fixed concentration of cisplatin (IC_{50}^{CisPt} on SCC-25: 10 µM),[28] and increasing concentrations of RuCy from 50 to 200 µM (IC_{50}^{RuCy} on SCC-25: 80 µM).[12] Different RuCy concentrations were assessed in order to observe a potential combinatorial effect of the two drugs on cells viability. To determine the combined effect, the synergistic coefficient (α) has been calculated for combined CisPt/RuCy treatment compared to CisPt and RuCy alone by using:

$$\alpha = (SF^a \times SF^b)/SF^{ab}$$

where SF is the survival fraction, *a* is CisPt treatment alone, *b* is RuCy treatment alone and *ab* is the resulted combination. If α<1 the effects are antagonistic, if α=1 the effects are additive or null while if α>1 the effects are synergistic.[29] A synergistic effect was observed from 48h after the co-chemo treatment (**Figure S5**) and confirmed by the α values (**Table S1**).

In order to investigate a potential enhanced effect of the co-treatment associated to the inclusion of the drugs in a single nanoplatform, NAs-CisPt-RuCy were tested and compared on the same cell line (**Figure S6A**). Indeed, the inclusion of drugs in nanoparticles should promote their internalization by increasing their local concentration within the cells that usually results in an improved cytotoxic effect.[30] NAs-CisPt-RuCy contain cisplatin prodrug and RuCy at a concentration of 40 µM and 400 µM, respectively. The 1:10 ratio well-matches the IC_{50} ratio calculated for the single drugs used for the investigations regarding the molecular drugs. Surprisingly, NAs-CisPt-RuCy did not show cytotoxic effect on 2D SCC-25 cells (**Figure S6A**) except for a small decrease in viability at very high concentrations. This result can be ascribed to a possible irreversible interaction between the components of NAs, which prevents both drugs from exerting their cytotoxic effect on cells. In order to shed light on the potential interactions between RuCy and gold USNPs, NAs-RuCy (NAs loaded with RuCy and without gold USNPs) were tested on SCC-25. The viability data (**Figure S6B**) confirmed that NAs-RuCy had no cytotoxic effect on cells, suggesting a potential interaction between RuCy and the polymeric matrix. Since the ruthenium is released from NAs-RuCy in buffer (**Figure S4**), such interaction may be responsible for the degradation of RuCy that might impair its functionality or for the steady maintenance of an amount of RuCy in the cytosol that may stimulate the cellular metabolism.[8]

In order to exploit the features of both drugs for co-chemotherapy, another strategy has been investigated by applying NAs loaded with cisplatin (NAs-CisPt) in combination with molecular RuCy (**Figure 2A**). As expected, this approach resulted in a significant synergism (**Table 2**) from 24h after treatment with both RuCy concentrations (100 µM and 200 µM), confirming the combined treatment is particularly effective when cisplatin is loaded in NAs and RuCy is administrated as a free compound.

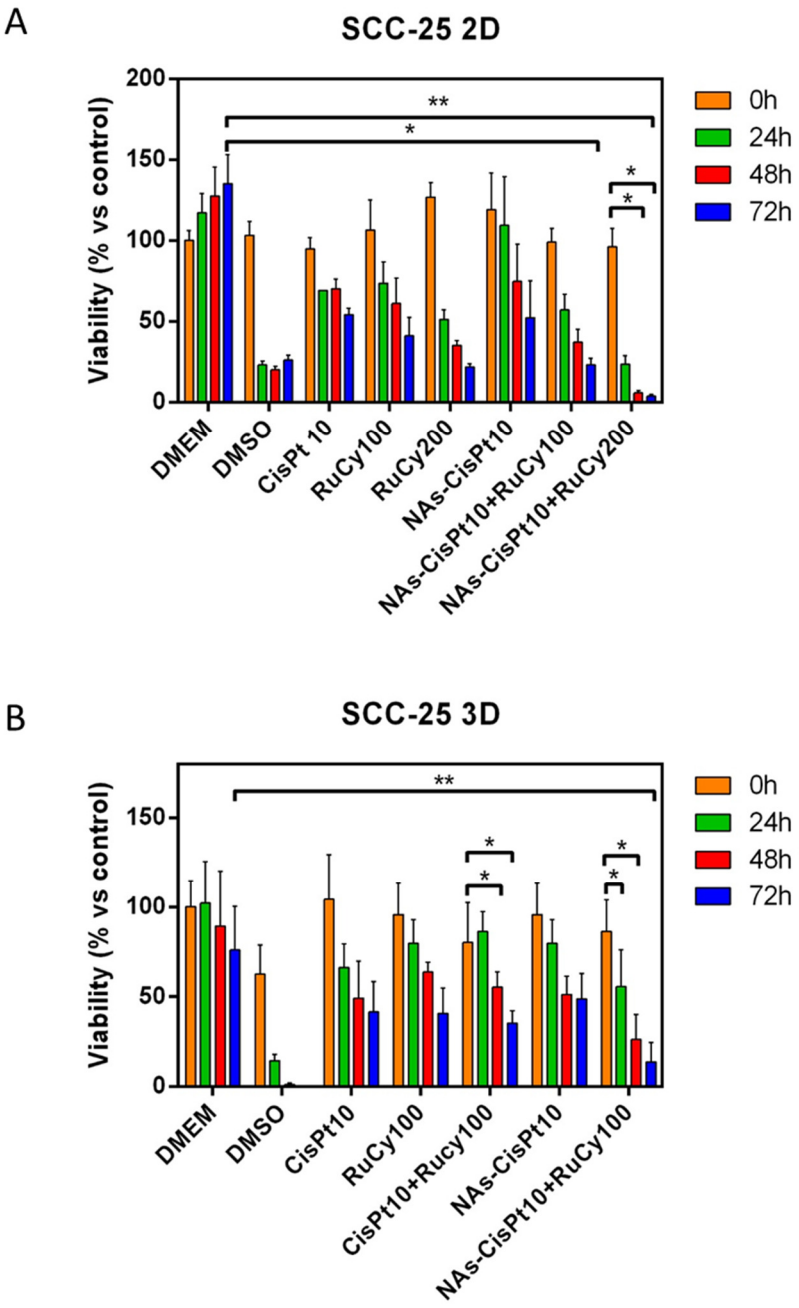

Figure 2: Viability assays on SCC-25. (**A**) Treatment of 2D cell cultures with NAs-CisPt at fixed concentration (10 µM in cisplatin prodrug) and two concentrations of RuCy co-administered as free drugs (100 µM and 200 µM). Cells were incubated with nanoparticles for 2h, then washed twice with PBS and viability was measured after 24, 48 and 72h. Viability measurements are normalized by the control (untreated cells - DMEM). Two-

way ANOVA with Turkey's multiple comparison test, *p ≤ 0,05 and **p ≤ 0.003. (**B**) Treatment of 3D cell cultures with fixed concentration of CisPt and Rucy (10 µM and 100 µM respectively) administered with different formulations. Spheroids were treated for 2h and then washed twice with PBS. Viability was measured compared to the control represented by cell not treated (DMEM). Two-way ANOVA with Turkey's multiple comparison test, *p ≤ 0,05 and **p ≤ 0.003. All results are obtained from 3 independent experiments and error bars state for standard deviation.

Table 2: Combined effect of NAs-CisPt and RuCy respect to treatments alone.

	24h	**48h**	**72h**
NAs-CisPt10 + RuCy100	1.1	1.1	0.9
NAs-CisPt10 + RuCy200	1.9	3.8	2.4

3.3 3D viability assay

In order to validate the data obtained on 2D cellular cultures, a more complex bio-model has been employed to evaluate the most promising co-chemo treatment approach. In this regard, multi-cellular tumor spheroids (MCTSs) represent an excellent platform for the progress of preclinical oncological investigations and the translation of nanomaterials to the clinics.[31] Indeed, MCTSs can mimic some features and complexity of both the tumor and the extracellular environment, and are widely used for drugs screening in agreement with the 3R's concept to reduce and optimize the use of animals.[32,33] The 3D spheroids of SCC-25 have been produced by a standardized protocol.[25] By taking into account the findings on 2D cellular cultures and the next *in vivo* evaluations, the spheroids have been treated with fixed concentration of the drugs (10 µM for CisPt and 100 µM of RuCy). MCTSs have been treated with the drugs for 2h, and then washed twice with PBS before measuring the viability. Significative differences in the viability of spheroids treated with the combination of the drugs have been observed (**Figure 2B**). Noticeably, a synergistic effect is appreciable only for the approach that comprise the employment of NAs-CisPt, while the use of free drugs results in an antagonistic effect (**Table 3**).

Table 3: Combined effect of NAs-CisPt and RuCy with respect to drugs alone on 3D spheroids.

	24h	**48h**	**72h**
CisPt10 + RuCy100	0.6	0.6	0.5
NAs-CisPt10 + RuCy100	1.1	1.2	1.4

3.4 CAM assay

The best combination of the treatments (NAs-CisPt+RuCy) has been finally evaluated by employing the chorioallantoic membrane (CAM) models, an optimized *in vivo* system that supports the formation of solid and vascularized tumors. The direct monitoring of tumor growth on CAM allows the reliable evaluation of the tumor-shrinking effects due to the therapeutic treatment applied as well as the cancer behaviors associated to the treatment response.[18] In this study, the potential antitumor effect of RuCy has been assessed as single or combined treatment with NAs-CisPt. Hence, at Embryonic Day of Development (EDD) 10, the tumor-bearing embryos have been randomized and divided into four groups: I) serum-free cell culture medium (control), II) RuCy, III) NAs-CisPt and IV) NAs-CisPt+RuCy. Tumors were monitored for four days following the application of the treatment and the volume was derived using a modified ellipsoid formula that considers the surface measurements of width and length (**Figure 4A**).[26] Overall, medium-treated tumors showed an increased tumor volume fold change both at EDD12 and 14 compared to the pretreatment tumor size at EDD10. By contrast, a progressive reduction of tumor fold change was observed for each treatment group between EDD10 and 14, suggesting that RuCy and NAs-CisPt promote tumor growth inhibition as both single and in combined administration (**Figure S7**). The comparison of the treatment conditions with each specific EDD to the control denotes an improved size reducing effect for both RuCy and NAs-CisPt+RuCy treated tumors compared to NAs-CisPt alone (**Figure 4B**) but without a clear additive effect.

Harvested tumors have been processed for the quantification of ruthenium, gold, and platinum content through ICP-MS analysis, which confirmed the accumulation of the metals in the tumors (**Figure 4C**). The results demonstrated a comparable accumulation of ruthenium in tumors treated with RuCy and co-treated with NAs-CisPt+RuCy (3.6% and 3.1%, respectively), confirming that the presence of NAs-CisPt does not affect the RuCy accumulation in cells. Interestingly, the biodistribution profile of ruthenium in embryo's organs was negligible, with %AD values lower than 0.05% (**Figure S8**). Moreover, the embryo viability was not significantly affected after the application of increasing dose of RuCy (25, 50 and 100 μg) (**Figure S9**). Taken together, these findings suggest the biosafety of RuCy for *in vivo* application. Further biological investigations are needed to reach a proper synergistic effect between RuCy and NAs-CisPt on the regulation of the major cancer-promoting mechanisms.

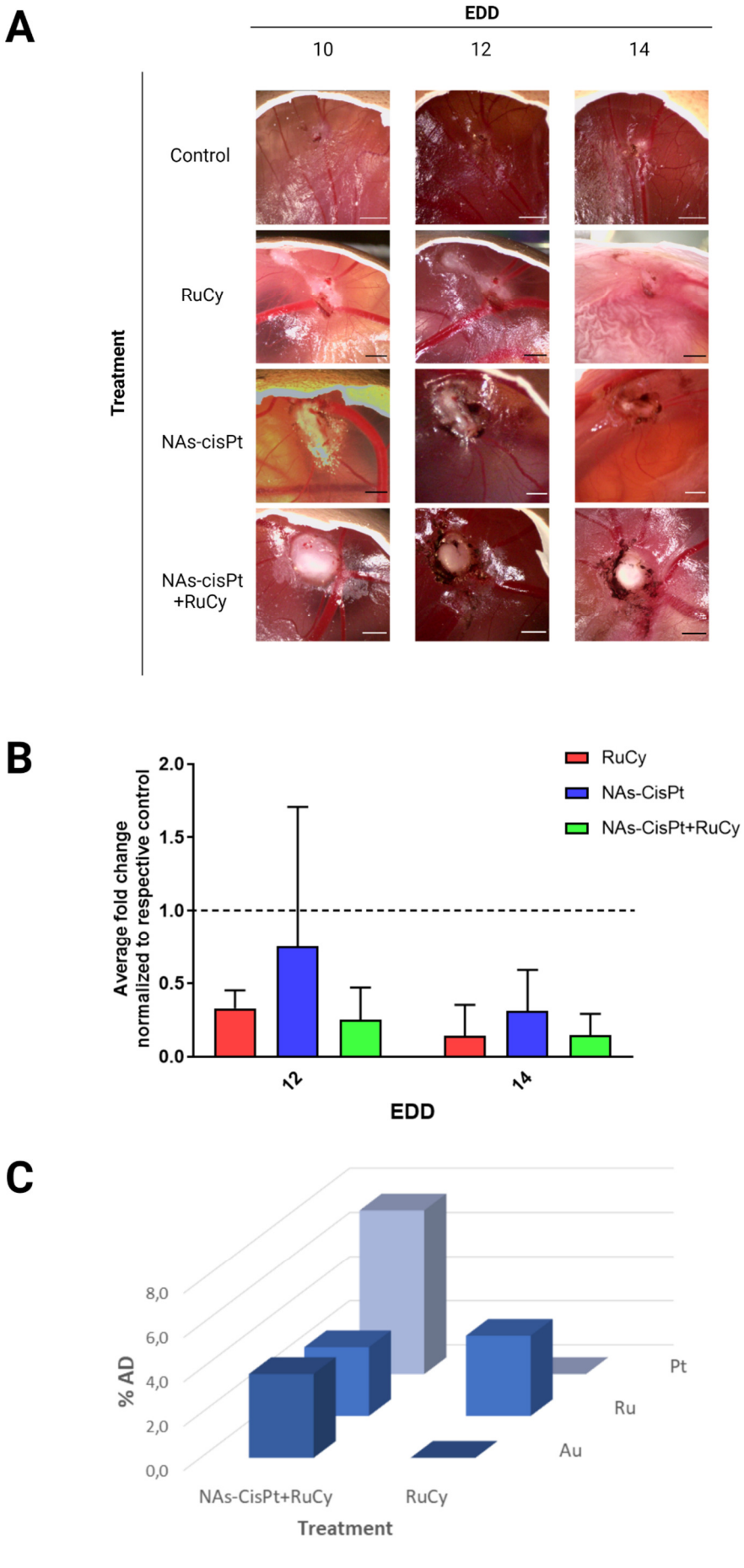
A
EDD
10
12
14
Treatment
Control
RuCy
NAs-cisPt
NAs-cisPt
+RuCy
B
RuCy
NAs-CisPt
NAs-CisPt+RuCy
Average fold change
normalized to respective control
2.0
1.5
1.0
0.5
0.0
12
14
EDD
C
8,0
6,0
4,0
2,0
0,0
% AD
Pt
Ru
Au
NAs-CisPt+RuCy
RuCy
Treatment

Figure 4: Evaluation of the antitumor effect of RuCy and NAs-CisPt on CAM. A) Representative images of tumor-bearing eggs on EDD10 (pre-treatment), EDD12 and EDD14. Scale bars: 2 mm. B) Tumor volume fold change of each treatment condition calculated over control at each respective EDD. C) ICP-MS quantification of ruthenium, gold and platinum in harvested tumors. The amount of metals are reported as % Administered Dose (%AD) with at least 3 samples per condition.

4. CONCLUSIONS

An emerging ruthenium complex (RuCy) has been successfully (co)loaded inside NAs demonstrating that multiple chemotherapeutics can be inserted into the nano-architectures. A supra-additive action has been observed in both 2D and 3D models by the combination of NAs-CisPt with free RuCy. This finding is of particular interest as the reduction of the cisplatin administered dose in patients can significantly reduce the associated side effects, by resulting in a better prognosis. The evaluations in CAMs confirmed the promising antitumor activity of RuCy on developing organisms and evidenced its biosafety and the lack of ruthenium bioaccumulation in major organs, while *in vitro* supra-additive effect was not corroborated. Our data confirm that the employment of alternative *in vivo* models is pivotal in oncological preclinical research to validate the *in vitro* findings within the 3R's concept, unveil the molecular mechanism involved in cancer treatment response, and finally promote the advancement of innovative approaches into the clinic. The exploitation of gold USNPs in NAs may result in the potential employment of multi-drug-loaded NAs in combination with photothermal- or radio-therapy for an integrated cancer management.[34,35] Overall, this work leads off to the development of the next strategies for the treatment of oral malignancies based on nano-structured co-chemotherapeutics.

Declaration of Competing Interest

The Authors declare no competing financial interests that could have appeared to influence the work reported in this paper.

Acknowledgment

The research leading to these results has received funding from AIRC under MFAG 2017 – ID 19852 project – P. I. Voliani Valerio.

Notes

Data processed and graphs prepared by using GraphPad Prism software (version 8.0). The raw and processed data required to reproduce these findings are available on request to the Authors. The graphical abstract was created with BioRender.com

Authors' contribution

M.S., V.F., cellular experiments and data analysis; V.F., M.L.E., A.K.M., A.Z., nano-architectures synthesis and characterizations, and ICP-MS quantification; P.S., A.G, N.G., V.F., A.K.M., A.Z., *in vivo* experiments and data analysis; L.B., synthesis and characterizations of the metal complexes; F.M. coordination of the metal complexes synthesis and characterizations; V.V., design and coordination of the project. All Authors have discussed the data and contributed to write the manuscript.

REFERENCES

[1] P. Bose, N.T. Brockton, J.C. Dort, Head and neck cancer: From anatomy to biology, Int. J. Cancer. 133 (2013) 2013–2023. https://doi.org/10.1002/ijc.28112.

[2] F. dos S. Menezes, G.A. Fernandes, J.L.F. Antunes, L.L. Villa, T.N. Toporcov, Global incidence trends in head and neck cancer for HPV-related and -unrelated subsites: A systematic review of population-based studies, Oral Oncol. 115 (2021) 105177. https://doi.org/10.1016/J.ORALONCOLOGY.2020.105177.

[3] H. Sung, J. Ferlay, R.L. Siegel, M. Laversanne, I. Soerjomataram, A. Jemal, F. Bray, Global Cancer Statistics 2020: GLOBOCAN Estimates of Incidence and Mortality Worldwide for 36 Cancers in 185 Countries, CA. Cancer J. Clin. 71 (2021) 209–249. https://doi.org/10.3322/CAAC.21660.

[4] D.E. Johnson, B. Burtness, C.R. Leemans, V.W.Y. Lui, J.E. Bauman, J.R. Grandis, Head and neck squamous cell carcinoma, Nat. Rev. Dis. Prim. 2020 61. 6 (2020) 1–22. https://doi.org/10.1038/s41572-020-00224-3.

[5] J.D. Cramer, B. Burtness, Q.T. Le, R.L. Ferris, The changing therapeutic landscape of head and neck cancer, Nat. Rev. Clin. Oncol. 2019 1611. 16 (2019) 669–683. https://doi.org/10.1038/s41571-019-0227-z.

[6] L.Q.M. Chow, Head and Neck Cancer, N. Engl. J. Med. 382 (2020) 60–72. https://doi.org/10.1056/NEJMRA1715715.

[7] J. Gao, Z. Wang, J. Fu, J. A., Y. Ohno, C. Xu, Combination treatment with cisplatin, paclitaxel and olaparib has synergistic and dose reduction potential in ovarian cancer cells, Exp. Ther. Med. 22 (2021) 1–9. https://doi.org/10.3892/ETM.2021.10367.

[8] U. Ndagi, N. Mhlongo, M.E. Soliman, Metal complexes in cancer therapy – an update from drug design perspective, Drug Des. Devel. Ther. 11 (2017) 599. https://doi.org/10.2147/DDDT.S119488.

[9] B.S. Murray, M. V. Babak, C.G. Hartinger, P.J. Dyson, The development of RAPTA compounds for the treatment of tumors, Coord. Chem. Rev. 306 (2016) 86–114. https://doi.org/10.1016/j.ccr.2015.06.014.

[10] A. Weiss, R.H. Berndsen, M. Dubois, C. Müller, R. Schibli, A.W. Griffioen, P.J. Dyson, P. Nowak-Sliwinska, In vivo anti-tumor activity of the organometallic ruthenium(ii)-arene complex [Ru(η6-p-cymene)Cl2(pta)] (RAPTA-C) in human ovarian and colorectal carcinomas, Chem. Sci. 5 (2014) 4742–4748. https://doi.org/10.1039/c4sc01255k.

[11] M. Rausch, P.J. Dyson, P. Nowak-Sliwinska, Recent Considerations in the Application of RAPTA-C for Cancer Treatment and Perspectives for Its Combination with Immunotherapies, Adv. Ther. 2 (2019) 1900042. https://doi.org/10.1002/ADTP.201900042.

[12] M. Santi, A.K. Mapanao, L. Biancalana, F. Marchetti, V. Voliani, Ruthenium arene complexes in the treatment of 3D models of head and neck squamous cell carcinomas, Eur. J. Med. Chem. 212 (2021) 113143. https://doi.org/10.1016/J.EJMECH.2020.113143.

[13] L. Biancalana, L.K. Batchelor, G. Ciancaleoni, S. Zacchini, G. Pampaloni, P.J. Dyson, F. Marchetti, Versatile coordination of acetazolamide to ruthenium(II) p-cymene complexes and preliminary cytotoxicity studies, Dalt. Trans. 47 (2018) 9367–9384. https://doi.org/10.1039/c8dt01555d.

[14] L. Biancalana, L.K. Batchelor, T. Funaioli, S. Zacchini, M. Bortoluzzi, G. Pampaloni, P.J. Dyson, F. Marchetti, α-Diimines as Versatile, Derivatizable Ligands in Ruthenium(II) p-Cymene Anticancer Complexes, Inorg. Chem. 57 (2018) 6669–6685. https://doi.org/10.1021/acs.inorgchem.8b00882.

[15] N. Joksimović, N. Janković, J. Petronijević, D. Baskić, S. Popovic, D. Todorović, M. Zarić, O. Klisurić, M. Vraneš, A. Tot, Z. Bugarčić, Synthesis, Anticancer Evaluation and Synergistic Effects with cis platin of Novel Palladium Complexes: DNA, BSA Interactions and Molecular Docking Study , Med. Chem. (Los. Angeles). 16 (2019) 78–92. https://doi.org/10.2174/1573406415666190128095732.

[16] D. Cassano, D.R. Martir, G. Signore, V. Piazza, V. Voliani, Biodegradable hollow silica nanospheres containing gold nanoparticle arrays, Chem. Commun. 51 (2015) 9939–9941. https://doi.org/10.1039/C5CC02771C.

[17] A.K. Mapanao, M. Santi, P. Faraci, V. Cappello, D. Cassano, V. Voliani, Endogenously Triggerable Ultrasmall-in-Nano Architectures: Targeting Assessment on 3D Pancreatic Carcinoma Spheroids, ACS Omega. 3 (2018) 11796–11801. https://doi.org/10.1021/ACSOMEGA.8B01719/SUPPL_FILE/AO8B01719_LIVESLIDES.MP4.

[18] P. Sarogni, A.K. Mapanao, A. Gonnelli, M.L. Ermini, S. Marchetti, C. Kusmic, F. Paiar, V. Voliani, Chorioallantoic membrane tumor models highlight the effects of cisplatin compounds in oral carcinoma treatment, IScience. 25 (2022) 103980. https://doi.org/10.1016/J.ISCI.2022.103980.

[19] A.K. Mapanao, G. Giannone, M. Summa, M.L. Ermini, A. Zamborlin, M. Santi, D. Cassano, R. Bertorelli, V. Voliani, Biokinetics and clearance of inhaled gold ultrasmall-in-nano architectures, Nanoscale Adv. 2 (2020) 3815–3820. https://doi.org/10.1039/D0NA00521E.

[20] A. Zamborlin, M.L. Ermini, M. Summa, G. Giannone, V. Frusca, A.K. Mapanao, D. Debellis, R. Bertorelli, V. Voliani, The Fate of Intranasally Instilled Silver Nanoarchitectures, Nano Lett. 22 (2022) 5269–5276. https://doi.org/10.1021/ACS.NANOLETT.2C01180.

[21] A.K. Mapanao, P.P. Che, P. Sarogni, P. Sminia, E. Giovannetti, V. Voliani, Tumor grafted – chick chorioallantoic membrane as an alternative model for biological cancer research and conventional/nanomaterial-based theranostics evaluation, Https://Doi.Org/10.1080/17425255.2021.1879047. 17 (2021) 947–968. https://doi.org/10.1080/17425255.2021.1879047.

[22] P. Sarogni, A.K. Mapanao, S. Marchetti, C. Kusmic, V. Voliani, A Standard Protocol for the Production and Bioevaluation of Ethical in Vivo Models of HPV-Negative Head and Neck Squamous Cell Carcinoma, ACS Pharmacol. Transl. Sci. 4 (2021) 1227–1234. https://doi.org/10.1021/ACSPTSCI.1C00083/ASSET/IMAGES/ACSPTSCI.1C00083.SOCIAL.JPEG_V03.

[23] M.D. Hall, C.T. Dillon, M. Zhang, P. Beale, Z. Cai, B. Lai, A.P.J. Stampfl, T.W. Hambley, The cellular distribution and oxidation state of platinum(II) and platinum(IV) antitumour complexes in cancer cells, JBIC J. Biol. Inorg. Chem. 8 (2003) 726–732. https://doi.org/10.1007/s00775-003-0471-6.

[24] S. Dhar, W.L. Daniel, D.A. Giljohann, C.A. Mirkin, S.J. Lippard, Polyvalent Oligonucleotide Gold Nanoparticle Conjugates as Delivery Vehicles for Platinum(IV) Warheads, J. Am. Chem. Soc. 131 (2009) 14652–14653. https://doi.org/10.1021/ja9071282.

[25] M. Santi, A.K. Mapanao, V. Cappello, V. Voliani, Production of 3D tumor models of head and neck

squamous cell carcinomas for nanotheranostics assessment, ACS Biomater. Sci. Eng. 6 (2020) 4862–4869. https://doi.org/10.1021/ACSBIOMATERIALS.0C00617/SUPPL_FILE/AB0C00617_LIVESLIDES.MP4.

[26] M. Rovithi, A. Avan, N. Funel, L.G. Leon, V.E. Gomez, T. Wurdinger, A.W. Griffioen, H.M.W. Verheul, E. Giovannetti, Development of bioluminescent chick chorioallantoic membrane (CAM) models for primary pancreatic cancer cells: a platform for drug testing, Sci. Reports 2017 71. 7 (2017) 1–13. https://doi.org/10.1038/srep44686.

[27] D. Cassano, J. David, S. Luin, V. Voliani, Passion fruit-like nano-architectures: a general synthesis route, Sci. Reports 2017 71. 7 (2017) 1–9. https://doi.org/10.1038/srep43795.

[28] M. Santi, A.K. Mapanao, D. Cassano, Y. Vlamidis, V. Cappello, V. Voliani, Endogenously-Activated Ultrasmall-in-Nano Therapeutics: Assessment on 3D Head and Neck Squamous Cell Carcinomas, Cancers (Basel). 12 (2020) 1063. https://doi.org/10.3390/cancers12051063.

[29] A.J. Trinidad, S.J. Hong, Q. Peng, S.J. Madsen, H. Hirschberg, Combined concurrent photodynamic and gold nanoshell loaded macrophage-mediated photothermal therapies: An *in vitro* study on squamous cell head and neck carcinoma, Lasers Surg. Med. 46 (2014) 310–318. https://doi.org/10.1002/LSM.22235.

[30] K. Cho, X. Wang, S. Nie, Z. (Georgia) Chen, D.M. Shin, Therapeutic Nanoparticles for Drug Delivery in Cancer, Clin. Cancer Res. 14 (2008) 1310–1316. https://doi.org/10.1158/1078-0432.CCR-07-1441.

[31] A.K. Mapanao, V. Voliani, Three-dimensional tumor models: Promoting breakthroughs in nanotheranostics translational research, Appl. Mater. Today. 19 (2020) 100552. https://doi.org/10.1016/J.APMT.2019.100552.

[32] M.A.G. Barbosa, C.P.R. Xavier, R.F. Pereira, V. Petrikaitė, M.H. Vasconcelos, 3D Cell Culture Models as Recapitulators of the Tumor Microenvironment for the Screening of Anti-Cancer Drugs, Cancers 2022, Vol. 14, Page 190. 14 (2021) 190. https://doi.org/10.3390/CANCERS14010190.

[33] T. Rodrigues, B. Kundu, J. Silva-Correia, S.C. Kundu, J.M. Oliveira, R.L. Reis, V.M. Correlo, Emerging tumor spheroids technologies for 3D *in vitro* cancer modeling, Pharmacol. Ther. 184 (2018) 201–211. https://doi.org/10.1016/J.PHARMTHERA.2017.10.018.

[34] P.P. Che, A.K. Mapanao, A. Gregori, M.L. Ermini, A. Zamborlin, M. Capula, D. Ngadimin, B.J. Slotman, V. Voliani, P. Sminia, E. Giovannetti, Biodegradable Ultrasmall-in-Nano Architectures Loaded with Cisplatin Prodrug in Combination with Ionizing Radiation Induces DNA Damage and Apoptosis in Pancreatic Ductal Adenocarcinoma, Cancers 2022, Vol. 14, Page 3034. 14 (2022) 3034. https://doi.org/10.3390/CANCERS14123034.

[35] A.K. Mapanao, M. Santi, V. Voliani, Combined chemo-photothermal treatment of three-dimensional head and neck squamous cell carcinomas by gold nano-architectures, J. Colloid Interface Sci. 582 (2021) 1003–1011. https://doi.org/10.1016/j.jcis.2020.08.059.